Available online at www.sciencedirect.com
ScienceDirect
Ceramics International 35 (2009) 2123–2129
CERAMICS INTERNATIONAL
www.elsevier.com/locate/ceramint

Thermal cyclic behavior of glass–ceramic bonded thermal barrier coating on nimonic alloy substrate

S. Das [a,*], S. Datta [a], D. Basu [a], G.C. Das [b]

[a] Central Glass and Ceramic Research Institute, 196, Raja S.C. Mullick Road, Kolkata 700032, India
[b] Department of Metallurgical and Material Engineering, Jadavpur University, Kolkata 700032, India

Received 18 August 2008; received in revised form 5 September 2008; accepted 20 November 2008
Available online 13 January 2009

Abstract

Thermal barrier coating system comprised of 8 wt.% yttria stabilized zirconia (YSZ) top coat, glass–ceramic bond coat and nimonic alloy (AE 435) substrate was subjected to thermal shock test from 1000 °C to room temperature for 100 cycles. Two types of thermal shock testing were performed. In one test, specimens held at 1000 °C for 5 min were forced air quenched while in the other test specimens were water quenched from the same conditions. Microstructural changes were investigated by scanning electron microscopy (SEM) and phase analysis was conducted by XRD and energy dispersive X-ray (EDX) analysis. In the case of forced air quenched specimens, no deterioration was observed in the top coats after 100 cycles while the top coats were damaged in the water quenched ones. In both forced air quenched and water quenched specimens, interfacial crack was not observed at the top coat–bond coat and bond coat–substrate interfaces after thermal cycling experiments and the top coat maintained its phase stability.

Keywords: B. Microstructure-final; C. Thermal shock resistance; D. Glass ceramics; D. ZrO_2

1. Introduction

Thermal barrier coatings (TBCs) are applied on the advanced gas turbine and diesel engine components because the current application calls for increased thermodynamic efficiency due to higher operating temperatures with reduced cooling air requirements and at the same time increased lifetime of the metallic substrate due to lower surface temperature [1–4]. Generally, thermal barrier coating consists of a ceramic top coat, an oxidation resistant MCrAlY/PtAl based metallic bond coat and a metal substrate. Usually, 6–8 wt.% yttria stabilized zirconia (YSZ) is preferred as top coat because of its low thermal conductivity (2.2–2.9 W/m K) [5,6], excellent thermal shock resistance and relatively high coefficient of thermal expansion (11.0×10^{-6}/K) [5,7]. The MCrAlY bond coat protects the underlying metal substrate from high temperature oxidation and minimizes stresses originated from thermal expansion mismatch between the top coat and the substrate [8].

However, TBCs tend to spall when they are subjected to thermal cycling due to thermal stresses generated for the thermal expansion mismatch with the underneath metal substrate as well as the temperature gradients, residual stresses during deposition, phase transformations, progressive sintering of the ceramic top coat and corrosive and erosive attack of the environment. Thermal shock resistance of the plasma sprayed coatings can be increased by enhancing the strain tolerance of the ceramic coating and by reducing the harmful residual stresses. The ceramic coating microstructure with controlled porosity, micro-cracks and segmentation cracks imparts high resistance to the degradation of the coating due to thermal cycling [9].

The intermediate bond coat layer with higher thermal expansion coefficient softens at the operating interfacial temperature, which in turn accommodates the stresses to some extent and reduces chances of the top coat spallation. However, with long time usage and increase in operating temperature, the bond coat undergoes phase transformation with associated change in volume and develops thermally grown oxide (TGO) layer in the interface with the top coat leading to enormous residual stresses, which often promotes failure of the thermal barrier coating system [10]. To overcome this

* Corresponding author. Tel.: +91 33 2473 3469/76/77/96; fax: +91 33 2473 0957.
E-mail address: sumana@cgcri.res.in (S. Das).

0272-8842/$34.00
doi:10.1016/j.ceramint.2008.11.025

problem, glass–ceramic material has been used as oxidation resistant bond coat between the YSZ top coat and the nimonic alloy substrate and thereby, eliminating degeneration of the TBC system due to oxidation of the bond coat [11].

The present investigation was conceived with the objective to study the thermal shock behavior of a TBC system consisting of YSZ top coat, glass–ceramic bond coat and nimonic alloy substrate. Microstructural and phase studies were carried out for the specimens exposed to severe thermal shock conditions.

2. Experimental

2.1. Materials

The thermal barrier coating composed of a glass–ceramic bond coat and a ceramic top coat was applied onto a nickel based superalloy substrate, nimonic alloy (AE 435, 20 mm × 20 mm × 2 mm). The nominal composition of the substrate is given in Table 1. The glass powder used for the bond coating had particle size of about 3–5 μm. The composition of the glass is shown (in wt.%) in Table 2.The top coating material was ceramic powder with a particle size of 35 ± 10 μm and chemical composition of 92 ZrO_2–8Y_2O_3 (YSZ), wt.%.

2.2. Deposition process

The bond coating material was prepared by melting the glass-forming batch at 1400 °C for 2 h and quenching the melt to yield the glass frit. The frit was crushed and then milled along with various mill additions e.g. fume silica – 3.0–5.0 (wt.%); washed Cr_2O_3 – 4.0–5.0 (wt.%); cobalt oxide – 0.3–0.5 (wt.%) and water in a porcelain ball mill for 48 h. Fine glass particles (3–5 μm) were obtained after wet milling. A thick paint like slurry of glass was prepared to apply over the cleaned metal surface. The surface of the nimonic alloy substrate was thoroughly prepared by thermal degreasing at 600 °C for 10 min in an oxidizing atmosphere, sand blasting and finally, ultrasonically cleaning with acetone for 15 min. Sand blasting was done on the surface of the substrate by a sand blasting machine using compressed air (pressure range – 125–140 kg/cm^2) to eject a high-speed stream of sand particles (20 mesh size) from a nozzle (outer diameter – 22 mm, inner diameter – 18 mm). After sand blasting, the surface roughness (R_a) of the nimonic alloy substrate was ∼2.23 μm. The glass slurry was applied on the cleaned substrates by conventional spraying technique. The glass powder coated substrates were dried at 100 °C for 45 min and subsequently fired at 1200 °C for 5 min in a muffle furnace to obtain continuous, impervious glass coating. The glass coated substrates were further heat treated at 1000 °C for 1 h to convert the glass coating to a glass–ceramic coating containing crystalline phases such as barium magnesium silicate and barium silicate. Thickness of the glass–ceramic bond coat was kept at ∼100 ± 10 μm. 8 wt.% YSZ was air plasma sprayed onto the glass–ceramic coated nimonic alloy substrates using a METCO-F4 plasma gun. The spraying parameters of the YSZ top coat are given in Table 3. The YSZ top coat was of ∼400 ± 20 μm thickness.

Table 1
Nominal composition of nimonic superalloy (AE 435).

Elements	wt.%
Cr	19–22
Fe	1.0
C	0.12
Si	0.8
Mn	0.7
Ti	0.15–0.35
Al	0.15
Cu	0.07
S	0.01
P	0.015
Ni	Balance

Table 2
Composition of glass frit.

Composition	wt.%
SiO_2	45
BaO	45
CaO	3
MgO	3
ZnO	2
MoO_3	2

2.3. Thermal shock test

Thermal shock test was conducted by two different methods using a muffle furnace. In one method, specimens were put into the furnace when the temperature of the furnace reached 1000 °C, held for 5 min and then forced air quenched from 1000 °C to room temperature. In the other method, specimens were water quenched after 5 min holding at 1000 °C. The sample weight was measured after each 10 cycles in both the cases. Five numbers of samples were used in each test. These types of thermal shock testing were already adopted by others [9,12,13]. Here, these methods were followed to compare the performance of the present TBC system with the conventional TBC system.

2.4. Microstructure and phase study

The samples were precisely cut at right angles to their lengths using a diamond wafering blade (Isomet, Buchler, USA). Some samples were slightly polished for the

Table 3
Spraying parameters of YSZ top coat.

Powder injection	Outside nozzle 6 mm
Power input (kW)	40
Primary/secondary gas in the plasma (standard l/min)	35 Ar/10 H_2
Carrier gas (Ar) flow in the feeder nozzle (standard l/min)	2.6
Stand-off distance (mm)	120

microstructural investigation by scanning electron microscopy (SEM, LEO S430i, LEO, UK). The cutting and polishing of the samples were done very carefully in order to avoid all possible damages to the coatings. Phase identification was carried out by X-ray diffractrometry (PW 1710, Philips Research Laboratory, Eindhoven, Netherlands). Elemental analysis was performed by energy dispersive X-ray analysis technique (EDX, SiLi detector). The nimonic alloy substrate was detached by dissolving the glass–ceramic bond coat in 40% HCl to examine the phase changes in the substrate surface, which was attached with the bond coat.

3. Results and discussion

3.1. Weight change

During forced air quench thermal shock test, the spallation of the YSZ top coat was not observed in the samples. However, the nimonic alloy substrate was oxidized during the quenching operation. Thus, the weight gain was observed in the forced air quenched samples up to 100 cycles due to oxidative weight gain of the substrate metal. On the contrary, the spallation of the YSZ top coat was observed in the samples during water quenching that predominated over the oxidation of nimonic alloy substrate. Therefore, the samples lost weight in the water quench thermal shock test up to 100 cycles [9]. In the case of forced air quenched samples, the weight gain was ~0.0016 g after 100 cycles (Fig. 1a) while in the water quenching test, the samples lost weight ~0.0324 g within 100 cycles (Fig. 1b). Nusair Khan and Lu [9] utilized these methods of thermal shock testing at 1020 °C for a TBC system consisting of a $93ZrO_2$–$7Y_2O_3$ top coat (300 ± 10 μm), a CoNiCrAlY bond coat (45 ± 10 μm) and a nickel based superalloy substrate (Hastelloy–X). In their case, initially both the forced air quenched and water quenched samples gained weight and then lost weight progressively. Initial weight gain of the samples occurred because of the oxidation of substrate and bond coat. The subsequent decrease in weight of the samples was due to ablation and spallation of the YSZ top coat. They showed that during forced air quenching and water quenching the weight loss of the samples was about 0.008 g and 0.16 g after 100 cycles, respectively.

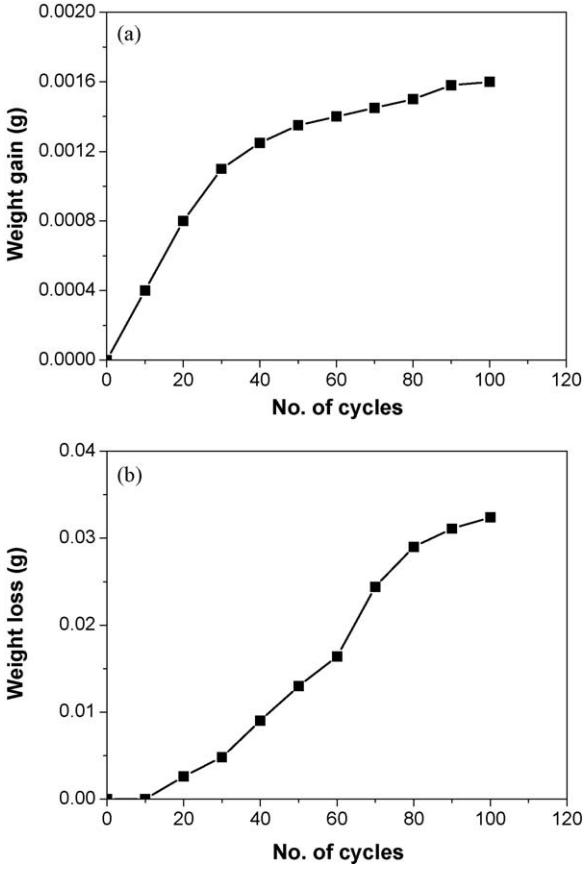

Fig. 1. (a) Weight gain during forced air quenching test and (b) weight loss during water quenching test.

3.2. Morphology of TBC

Fig. 2 depicts the cross-sectional micrograph of a typical as-deposited TBC system. It can be noticed from this figure that the interface between the glass–ceramic bond coat and the YSZ top coat is not visible. This indicates better structural integration of the TBC system. Furthermore, fine micro-cracks were observed in the as-deposited YSZ top coat. In the forced air quenched samples, no spallation and cracking were observed in the surfaces of the top coats after 100 cycles. For this reason, coating thickness remained the same after thermal cycling experiment (Fig. 3a and b). On the other hand, top coat surfaces were gradually deteriorated during thermal cycling in the water quenched samples. It was noted that the surfaces of the top coats were damaged after the thermal shock test for 100 cycles. Typical cross-sectional microstructures (Fig. 4a and b) illustrate that the surface and near surface regions of the top coat were damaged but still attached to the underlying region of the coating. Thus, the thickness of the top coat was not reduced. The progress of damage in the water quenched samples may be attributed to extension of micro-crack, micro-crack link up and thereafter large crack propagation [9]. However, the water quenched samples had

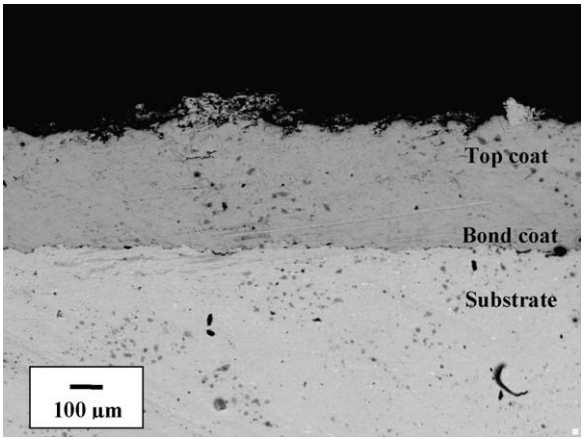

Fig. 2. As-deposited TBC system.

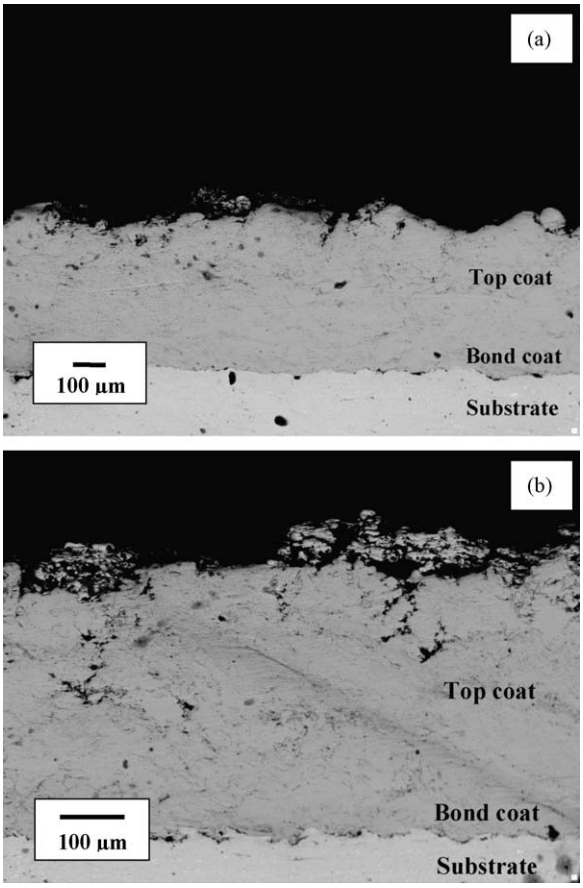

Fig. 3. (a) Typical cross-section microstructure of forced air quenched sample after 100 cycles and (b) magnified view of same sample.

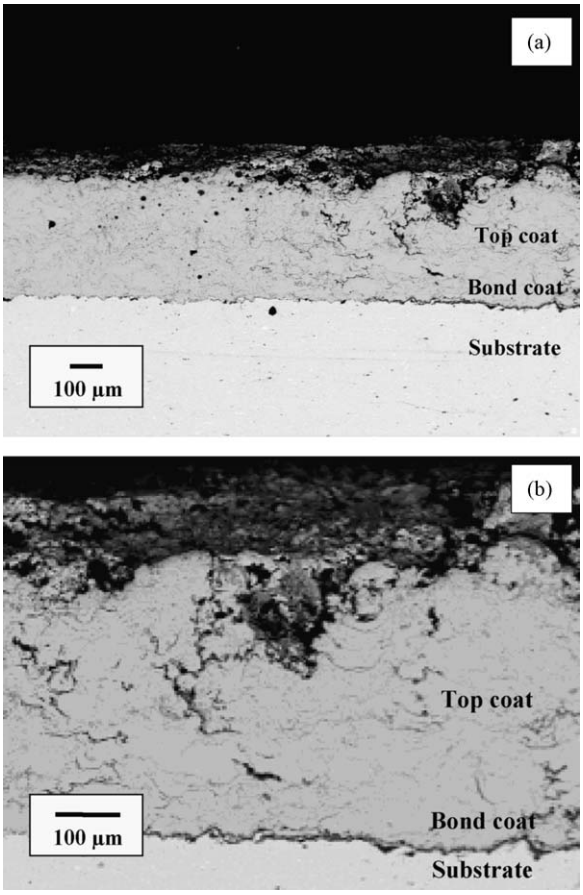

Fig. 4. (a) Typical cross-section microstructure of water quenched sample after 100 cycles and (b) magnified view of part (a).

high density of micro-cracks throughout the bond coats and the top coats. In addition, some large cracks were also found to be present in the bond coats and the top coats of the samples (Fig. 4a and b). In contrast, the air quenched samples showed only few numbers of micro-cracks in the bond coats and the top coats (Fig. 3a and b). Further, the top coat–bond coat and bond coat–substrate interfaces were free from any interfacial crack and the three layered structure remained intact even after these thermal shock treatments for 100 cycles (Figs. 3 and 4).

The thermal cyclic stresses encountered due to thermal expansion mismatch between the YSZ top coat and the nimonic alloy substrate and steep thermal gradient present in the TBC system did not affect the structures of the top coat and the bond coat because of high strain tolerance of the micro-cracked YSZ top coat and stress relaxation property of the glass–ceramic bond coat due to viscous flow of glass at the interfacial temperatures.

Nusair Khan and Lu [8] performed thermal shock test of a TBC system consisting of $93ZrO_2$–$7Y_2O_3$ top coat, CoNiCrAlY bond coat and stainless steel substrate using the same methods at 1020 °C. Thickness of the bond coat was 45 ± 10 μm whereas the top coat thickness was varied from 300 μm to 500 μm. They found that the thermal cycle life depends on the thickness of the top coat and for a thickness of 400 μm, the sustained cycles for forced air quenched and water quenched samples were only 29 and 15–18, respectively.

3.3. Oxidation resistance of bond coat

Bond coat oxidation is a detrimental phenomenon, which determines the lifetime of a conventional TBC system [10]. Therefore, TGO layer formation and its progressive growth should be controlled to minimize the bond coat oxidation induced TBC degradation. Since glass–ceramic bond coat is basically oxide based, bond coat oxidation did not occur during thermal cycling. Thus, TGO layer was not present between the bond coat and the top coat of the TBC system (Figs. 3 and 4). As a matter of fact, bond coat oxidation had no role in the present case. Rather, barium magnesium silicate based glass–ceramic bond coat protected the nimonic alloy substrate from high temperature oxidation quite satisfactorily. Fig. 5 demonstrates the oxidation behavior of bare nimonic alloy substrate and glass–ceramic coated nimonic alloy substrate at 1000 °C. After 100 h exposure to air, glass–ceramic coated nimonic alloy substrate had an oxidative weight gain of ~0.1 mg/cm^2 while in the case of bare nimonic alloy substrate the weight gain due to oxidation was ~0.69 mg/cm^2. The inherent lower thermal conductivity and high oxidation resistance of the glass–ceramic bond coat

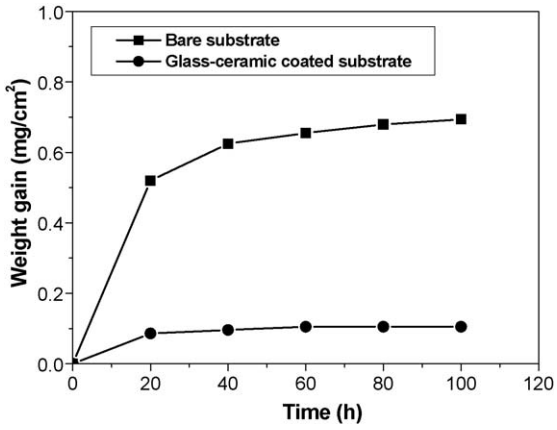

Fig. 5. Oxidative weight gain of nimonic alloy substrate and glass–ceramic coated nimonic alloy substrate at 1000 °C.

decreased the surface temperature of the nimonic alloy substrate and protected it from oxidation.

3.4. Bond coat–substrate interface region

During firing of the glass powder coated nimonic alloy substrate, substrate was oxidized by atmospheric oxygen leading to formation of an oxide scale on its surface before the glass powder started to melt and flow. Thereafter, the oxide scale was dissolved in the molten glass. Consequently, the activity of the substrate oxide was increased in the glass coating at the interface of coating and substrate. Thus, good adherence of the glass coating to the substrate was achieved because of the saturation of the coating with the substrate oxide at the interface [14].

In the as-sprayed TBC system, the oxide-rich transitional layer between the nimonic alloy substrate and the glass–ceramic bond coat was very thin (∼5 μm) and discontinuous along the interface (Fig. 6a). Even after thermal cycling for 100 cycles, the average thickness of this layer was not enhanced in the both forced air quenched and water quenched samples (Fig. 6b and c). However, it can be noted that the interfacial layer was discontinuous in the forced air quenched sample (Fig. 6b) whereas it was continuous in the water quenched sample (Fig. 6c). Furthermore, the transitional zone was slightly enlarged (∼10 μm) in the water quenched sample (Fig. 6c). During thermal cycling tests, the TBC systems were exposed to 1000 °C for 500 min in air. Hence, the transitional zone became continuous and extended in the water quenched sample because substrate metal was oxidized at the substrate–bond coat interface region due to presence of voids, large cracks and micro-cracks in the coating (Fig. 4a and b) that helped diffusion of oxygen through the coating. However, thermal exposure of the TBC system did not influence the substrate metal oxidation of the air quenched sample because only few micro-cracks were present in the coating (Fig. 3a and b), which did not assist the diffusion of oxygen. The gray regions at the bond coat–substrate interfaces (Fig. 6a and b) were identified as Cr_2O_3 by the X-ray diffraction analysis of the metallic substrates of forced air quenched and water quenched samples (Fig. 7a and b). EDX analysis (Fig. 8a and b) at the gray regions

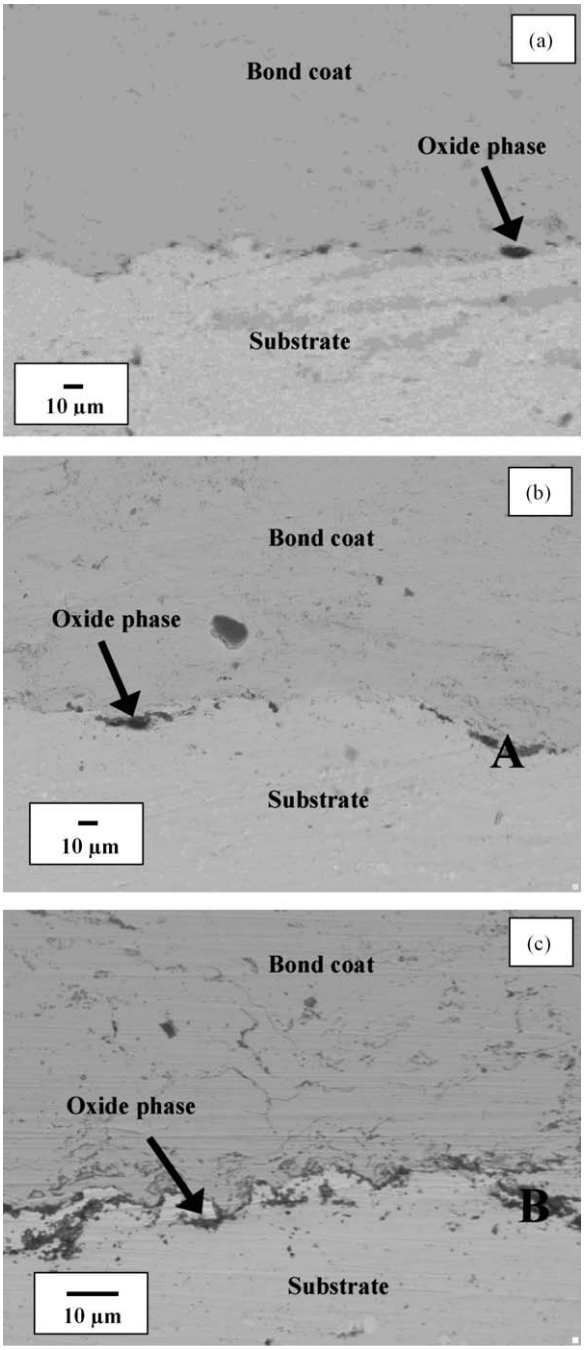

Fig. 6. Bond coat–substrate interface regions of (a) as-deposited sample; (b) forced air quenched sample after 100 cycles and (b) water quenched sample after 100 cycles.

indicated as A and B in Fig. 6a and b, respectively, confirmed the XRD results.

Tomsia and Pask [15] reported the bonding of K-alumino-silicate glass to commercial 80Ni–20Cr alloy. They studied that pre-oxidation treatment generated a single layer scale of Cr_2O_3 and NiO with the outer portion richer in Cr_2O_3. Good quality coating was produced by subsequent sealing. Dissolution of oxide from the scale led to saturation of the glass coating with Cr_2O_3 at the interfacial region. Presence of Si considerably reduces the mobility of Ni relative to that of Cr. Similarly, in the

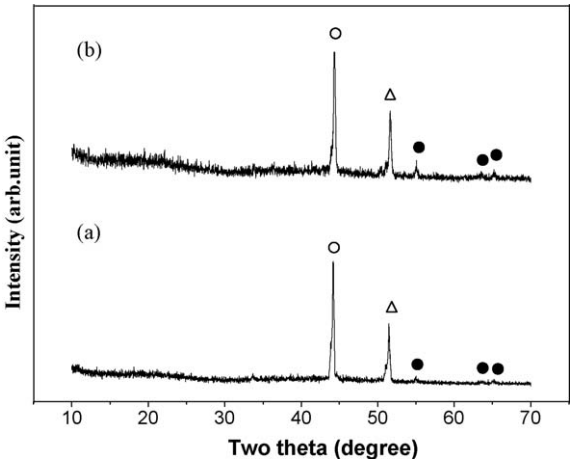

Fig. 7. XRD patterns for nimonic alloy substrates of (a) forced air quenched sample and (b) water quenched sample after 100 cycles. (○) Cr, (△) Ni, (●) Cr_2O_3.

present case, as silicon is present in the substrate alloy the mobility of Ni was reduced during firing treatment. Thus, Cr was oxidized by atmospheric oxygen resulting in Cr_2O_3. The reaction can be represented as follows [16]:

$$4/3Cr_{substrate} + O_2 = 2/3Cr_2O_3 \quad (1)$$

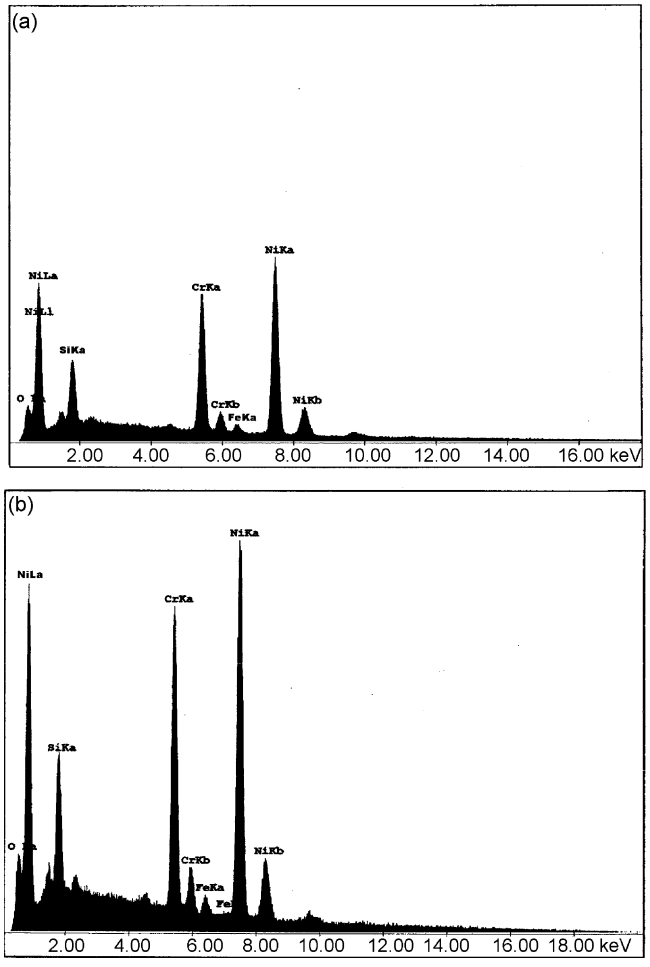

Fig. 8. EDX analysis at (a) region A of Fig. 6a and (b) region B of Fig. 6b.

Formation of Cr_2O_3 by reaction (1) increased the activity of Cr_2O_3 in the glass coating at the coating–substrate interface that enhanced the adherence of the coating due to saturation of the coating with Cr_2O_3 at the interface.

3.5. Phase stability of top coat

The plasma sprayed 6–8 wt.% yttria stabilized zirconia top coat contains maximum amount of the non-equilibrium and non-transformable tetragonal zirconia phase (t′). This t′ phase does not undergo the tetragonal (t) to monoclinic (m) transformation, which is deleterious due to large stress generation (volume expansion of ~4%). Accordingly, during thermal cycling the t′ phase is stable above and below the tetragonal to monoclinic transformation temperature (1170 °C). However, a cation diffusion controlled transformation of the t′ phase to the tetragonal (t) and cubic (c) equilibrium phases may occur during heat treatment at typical service temperatures. If this transformation takes place, then the tetragonal (t) phase transforms to the monoclinic phase and as a result of that, the lifetime of the TBC system is decreased [17].

XRD was done to find out any phase changes in the YSZ top coats after the thermal shock tests. XRD of as-sprayed YSZ coating identified only tetragonal zirconia (t′) phase (Fig. 9a). In the case of forced air quenched and water quenched samples, the top coat phase was stable even after 100 cycles. No peaks

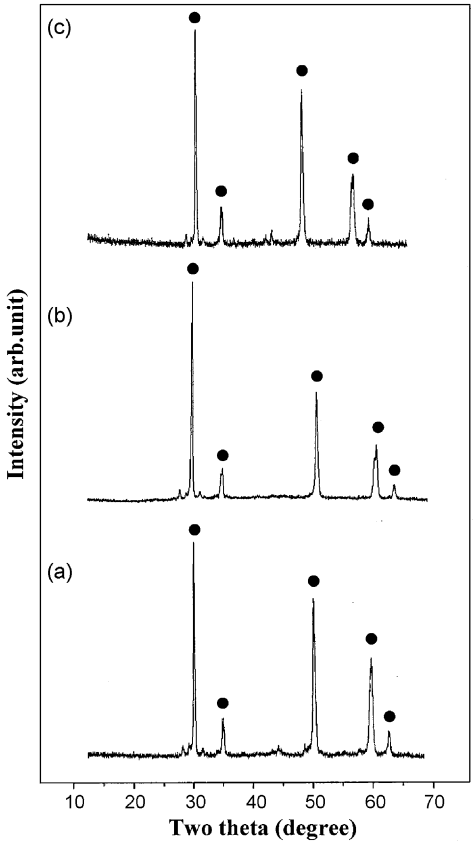

Fig. 9. Typical X-ray diffraction patterns for (a) as-sprayed sample; (b) forced air quenched sample after 100 cycles and (c) water quenched sample after 100 cycles. [(●) tetragonal zirconia (t′)].

other than tetragonal zirconia (t′) were detected to be present in the top coats (Fig. 9b and c). XRD result (Fig. 9c) indicates that during water quenching water has not reacted with YSZ top coat at 1000 °C. Nusair Khan and Lu have reported the same observation at 1020 °C [9]. Zhou et al. also showed that water vapor has no reaction with YSZ at 1050 °C [18].

4. Conclusions

The present TBC system with glass–ceramic based bond coat exhibited high thermal shock resistance. After thermal shock testing for 100 cycles, the top coat was not affected in the forced air quenched sample while deterioration of the top coat was observed at the surface and near surface regions in the water quenched sample. In the both cases, no horizontal or vertical cracking of the top coat and the bond coat and interface cracking were noticed. The two layered coating system was intimately bonded to the substrate even after the thermal shock tests for 100 cycles. Moreover, top coat phase stability was found in both forced air quenched and water quenched samples after 100 cycles. Thus, the present study indicates that the glass–ceramic material can be used as thermal shock resistant bond coat in a TBC system.

Acknowledgements

The authors are very grateful to Dr. H.S. Maiti, Director, Central Glass and Ceramic Research Institute, Kolkata 700 032, India, for his kind permission to publish this paper. The authors would like to thank Dr. (Mrs.) S. Sen, Mr. A.K. Mandal, Mrs. S. Roy, Dr. S. Majumder, Mr. A. Karmakar and Mr. B. Chakraborty for their assistance in doing SEM/EDX, XRD and other experiments, respectively.

References

[1] D. Basu, C. Funke, R.W. Steinbrech, Effect of heat treatment on elastic properties of separated thermal barrier coatings, Journal of Materials Research 14 (1999) 4643–4650.
[2] H. Chen, X. Zhou, C. Ding, Investigation of the thermomechanical properties of a plasma-sprayed nanostructured zirconia coating, Journal of the European Ceramic Society 23 (2003) 1449–1455.
[3] C. Ramachandra, K.N. Lee, S.N. Tewari, Durability of TBCs with a surface environmental barrier layer under thermal cycling in air and in molten salt, Surface & Coatings Technology 172 (2003) 150–157.
[4] A. Kulkarni, A. Vaidya, A. Goland, S. Sampath, H. Herman, Processing effects on porosity-property correlations in plasma sprayed yttria-stabilized zirconia coatings, Materials Science & Engineering A 359 (2003) 100–111.
[5] H. Zhao, F. Yu, T.D. Bennett, H.N.G. Wadley, Morphology and thermal conductivity of yttria-stabilized zirconia coatings, Acta Materialia 54 (2006) 5195–5207.
[6] J.R. Nicholls, K.J. Lawson, A. Johnstone, D.S. Rickerby, Methods to reduce the thermal conductivity of EB-PVD TBCs, Surface & Coatings Technology 151–152 (2002) 383–391.
[7] A.G. Evans, D.R. Mumm, J.W. Hutchingson, G.H. Meier, F.S. Pettit, Mechanisms controlling the durability of thermal barrier coatings, Progress in Materials Science 46 (2001) 505–553.
[8] A. Nusair Khan, J. Lu, Thermal cyclic behavior of air plasma sprayed thermal barrier coatings sprayed on stainless steel substrates, Surface & Coatings Technology 201 (2007) 4653–4658.
[9] A. Nusair Khan, J. Lu, Behavior of air plasma sprayed thermal barrier coatings, subject to intense thermal cycling, Surface & Coatings Technology 166 (2003) 37–43.
[10] M. Martena, D. Botto, P. Fino, S. Sabbadini, M.M. Gola, C. Badini, Modelling of TBC system failure: Stress distribution as a function of TGO thickness and thermal expansion mismatch, Engineering Failure Analysis 13 (2006) 409–426.
[11] S. Das, S. Datta, D. Basu, G.C. Das, Glass–ceramics as oxidation resistant bond coat in thermal barrier coating system, Ceramics International, in press, doi:10.1016/j.ceramint.2008.07.005.
[12] S.O. Chwa, A. Ohmori, Microstructures of ZrO_2-8 wt.%Y_2O_3 coatings prepared by a plasma laser hybrid spraying technique, Surface & Coatings Technology 153 (2002) 304–312.
[13] X.Q. Ma, M. Takemoto, Quantitative acoustic emission analysis of plasma sprayed thermal barrier coatings subjected to thermal shock tests, Materials Science & Engineering A 308 (2001) 101–110.
[14] I.W. Donald, Preparation, properties and chemistry of glass- and glass–ceramic-to-metal seals and coatings, Journal of Materials Science 28 (1993) 2841–2886.
[15] A.P. Tomsia, J.A. Pask, Bonding of dental glass to nickel–chromium alloys, Journal of the American Ceramic Society 69 (1986) C-239–C-240.
[16] C. Heald, A.C.K. Smith, Applied Physical Chemistry, The Macmillan Press Ltd., London and Basingstoke, 1974.
[17] P.A. Langjahr, R. Oberacker, M.J. Hoffmann, Long-term behavior and application limits of plasma-sprayed zirconia thermal barrier coatings, Journal of the American Ceramic Society 84 (2001) 1301–1308.
[18] C. Zhou, J. Yu, S. Gong, H. Xu, Influence of water vapor on the isothermal oxidation behavior of thermal barrier coatings, Journal of Materials Science & Technology 20 (2004) 38–40.